
[View Journal Online](#)  
[View Article Online](#)

## Computational approach for predicting the adsorption properties and inhibition of some antiretroviral drugs on copper corrosion in HNO<sub>3</sub>

Mougo André Tigori <sup>1,\*</sup>, Amadou Kouyaté <sup>1</sup>, Victorien Kouakou <sup>2</sup>, Paulin Marius Niamien <sup>2</sup> and Albert Trokourey <sup>2</sup>

<sup>1</sup> Unité de Formation et de Recherche Environnement, Université Jean Lorougnon Guédé, BP 150 Daloa, Côte d'Ivoire  
 tigori20@yahoo.fr (M.A.T.), amadoukyte@yahoo.fr (A.K.)

<sup>2</sup> Laboratoire de Chimie Physique, Université Félix Houphouët Boigny, 22 BP 582 Abidjan 22, Côte d'Ivoire  
 kmamphaili@yahoo.com (V.K.), niamienfr@yahoo.fr (P.M.N.), trokourey@gmail.com (A.T.)

\* Corresponding author at: Unité de Formation et de Recherche Environnement, Université Jean Lorougnon Guédé, BP 150 Daloa, Côte d'Ivoire.  
 e-mail: [tigori.mougo@ujlg.edu.ci](mailto:tigori.mougo@ujlg.edu.ci) (M.A. Tigori).

### RESEARCH ARTICLE



 10.5155/eurjchem.11.3.235-244.2011

Received: 24 July 2020

Received in revised form: 22 August 2020

Accepted: 23 August 2020

Published online: 30 September 2020

Printed: 30 September 2020

### KEYWORDS

Corrosion  
 Adsorption  
 Eco-friendly  
 Antiretroviral  
 Dual descriptor  
 Density functional theory

### ABSTRACT

The use of computational chemistry as an effective means of designing eco-friendly organic corrosion inhibitors has been greatly enhanced by the development of Density Functional Theory (DFT). In this study, the inhibitory activity of four antiretroviral drugs, namely, lamivudine, emtricitabine, didanosine and stavudine, was analyzed by this theory. The quantum chemical parameters/descriptors calculated using DFT at B3LYP/6-31G(d) level were used to explain the mechanism of electron transfer between the inhibitors and the copper surface. The results showed that these compounds adsorb on copper surface. It is important to consider the effect of films formed by the adsorption products. In addition, the Fukui functions and the dual descriptor were used as indicators to locate the electrophilic and nucleophilic attack sites within each compound. Finally, the DFT has enabled to accurately predict the adsorption properties and the good inhibition performance of the molecules in the solution studied.

Cite this: *Eur. J. Chem.* 2020, 11(3), 235-244

Journal website: [www.eurjchem.com](http://www.eurjchem.com)

### 1. Introduction

One of the most important challenges for practical and effective corrosion control today is the use of eco-friendly corrosion inhibitors. Inhibitors are used as an effective approach to increase the resistance of metals [1-4]. In general, copper is resistant to corrosion because of the formation of an oxide layer on its surface; however, the formation of scale and corrosion products is common in aggressive environments such as acidic, basic and saline environments [4]. Thus, to remove scale and corrosion products, acid cleaning is regularly carried out by industry [5]. This acid cleaning not only removes scale and corrosion products, but also accelerates the dissolution of the metal [6], which is why many researchers have paid particular attention to the search for corrosion inhibitors to support all metal users. It should be noted that the industry spends a lot of money each year to replace corroded metal structures. The focus of this research is on eco-friendly corrosion inhibitors that are less expensive and readily available. These eco-friendly inhibitors can be divided into two categories: organic and inorganic inhibitors. This issue has led

some researchers to use green corrosion inhibitors such as plant extracts [7,8] and drugs such as antibiotics drugs [9,10], opioid analgesics [11], antipsychotic drugs [12], antihypertensive drugs [13,14], amoebicidal drugs [15,16] and anti-biotics drugs [17].

To remain within this motivation, we have theoretically tested the inhibition properties of four antiretroviral molecules. Indeed, antiretroviral are inhibitors of the in vitro replication of the human immunodeficiency virus (HIV) in cultures of human cells and their lines. These molecules used to prevent and treat HIV/AIDS are therefore eco-friendly inhibitors and nontoxic and can reduce metal corrosion in aggressive environments. Some antiretroviral have been used as steel corrosion inhibitors [18,19]. According to the literature, some eco-friendly inhibitor organic compounds have been shown to have good inhibition performance in the corrosion of metals [20-23]. In addition, these organic compounds studied contain heteroatoms such as nitrogen, oxygen, or sulphur and/or  $\pi$ -electrons. They can adsorb on the copper surface forming a complex that isolates the metal from the aggressive medium [24,25].

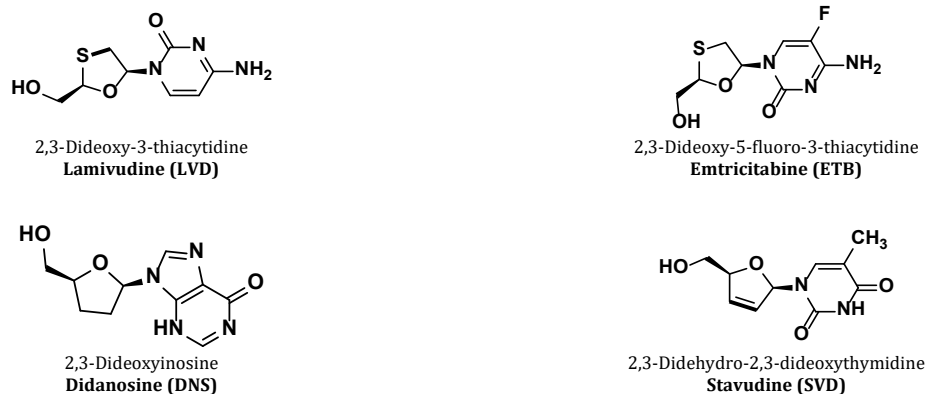


Figure 1. Chemical structures of studied molecules.

The complex that forms on the copper surface is formed either by physical or chemical adsorption or by a combination of both. Physical adsorption results from an electrostatic interaction between the ions or dipoles of the molecules and the surface of the electrically charged metal. Physical adsorption involves weak bonds, while chemical adsorption involves the transfer or sharing of electrons between the inhibitor molecules and the unsaturated "d" orbitals of the metal surface, resulting in the formation of covalent bonds (strong bonds). The different experimental techniques have allowed some authors to explain these different types of adsorption [26-29]. Although experimental techniques have been successful in capturing inhibition performance, they are expensive and time consuming. However, these techniques do not clearly explain the inhibition mechanism, which remains a mystery. That is why, in recent years, researchers have developed fast, efficient and less expensive techniques to predict the trend of inhibition ability of the inhibitors and to study the interactions that occur between adsorbed molecules and metal surfaces [30]. Quantum chemical calculations based on DFT have been used to achieve this goal as it is the practical way to determine the inhibition mechanism of compounds on metal surfaces [31-36].

The main objective of this study is to correlate the inhibition performance and quantum chemical parameters of the four antiretroviral molecules (Figure 1) to elucidate the mechanisms on copper corrosion inhibition in 1 M nitric acid solution.

## 2. Quantum chemical calculations

The quantum chemistry calculations were performed in gas phase using Gaussian 09 software [37]. These calculations are based on DFT method which is another approach to describe the fundamental state of molecular systems [38]. Its success stems from the fact that it can be applied to many systems (materials, organic molecules, complexes, carbon nanotubes, etc.) and its computation time is relatively lower than post-Hartree-Fock methods. Currently, it is used to describe metal-inhibitor interactions. DFT studies have been carried out for neutral and protonated forms for molecules and optimized using the hybrid functional B3LYP [39] (Beckes' three-parameter with Lee-Yang-Parr exchange correlation function) whose analytical form is given by:

$$E_{XC}^{B3LYP} = E_{XC}^{LDA} + a_0(E_X^{HF} - E_X^{LDA}) + a_x(E_X^{GGA} - E_X^{LDA}) + a_c(E_C^{GGA} - E_C^{LDA}) \quad (1)$$

$a_0 = 0.20$ ;  $a_x = 0.72$ ;  $a_c = 0.81$ ;  $E_{XC}^{LDA}$ : Exchange-correlation energy in Local Density Approximation;  $E_X^{HF}$ ,  $E_X^{LDA}$ ,  $E_X^{GGA}$  are exchange-energy in Hatree-Fock (HF), Local Density Approximation (LDA) and Generalized Gradient Approximation (GGA), respectively;  $E_C^{GGA}$ ,  $E_C^{LDA}$  are correlation energy in Generalized

Gradient Approximation (GGA) and Local Density Approximation (LDA), respectively.

These theoretical calculations which were based on 6-31G(d) basis set enabled access to computational global parameters, namely, the highest occupied molecular orbital energy ( $E_{HOMO}$ ), the lowest unoccupied molecular orbital energy ( $E_{LUMO}$ ), energy gap ( $\Delta E$ ), dipole moment ( $\mu$ ), the electron affinity (A), the ionization energy (I), the electronegativity ( $\chi$ ), the hardness ( $\eta$ ), the softness ( $\sigma$ ), the electrophilicity index ( $\omega$ ), the fraction of electron transferred ( $\Delta N$ ) and total energy (TE). The following parameters are determined using the equations shown below.

The energy gap is determined by the following relationship:

$$\Delta E = E_{LUMO} - E_{HOMO} \quad (2)$$

The ionization potential (I) and electron affinity (A) of the inhibitors are calculated according to Koopman's theorem [40]

$$I = -E_{HOMO} \quad (3)$$

$$A = -E_{LUMO} \quad (4)$$

The electronegativity ( $\chi$ ) [41] and the hardness ( $\eta$ ) [41] of the inhibitors were estimated using the value of I and A that given by:

$$\chi = -\mu_p = \left(\frac{\partial E}{\partial N}\right)_{v(r)} \quad (5)$$

$$\chi = \frac{I+A}{2} = -\frac{E_{LUMO} + E_{HOMO}}{2} \quad (6)$$

$$\eta = \frac{I-A}{2} = \frac{E_{LUMO} - E_{HOMO}}{2} \quad (7)$$

The global softness ( $\sigma$ ) is obtained from the equation [42]:

$$\sigma = \frac{1}{\eta} = \frac{2}{I-A} \quad (8)$$

The global electrophilicity index ( $\omega$ ) [41] is defined as follows:

$$\omega = \frac{\mu_p^2}{2\eta} = \frac{(I+A)^2}{4(I-A)} \quad (9)$$

In order to distinguish between situations of donation and acceptance of electrons or charges, new indicators from electron affinity and ionization potential have been introduced by José L. Gázquez *et al.* [43]. These indicators, which are electron acceptor ability ( $\omega^+$ ) and electron donor ability ( $\omega^-$ ) are given by the following expressions:

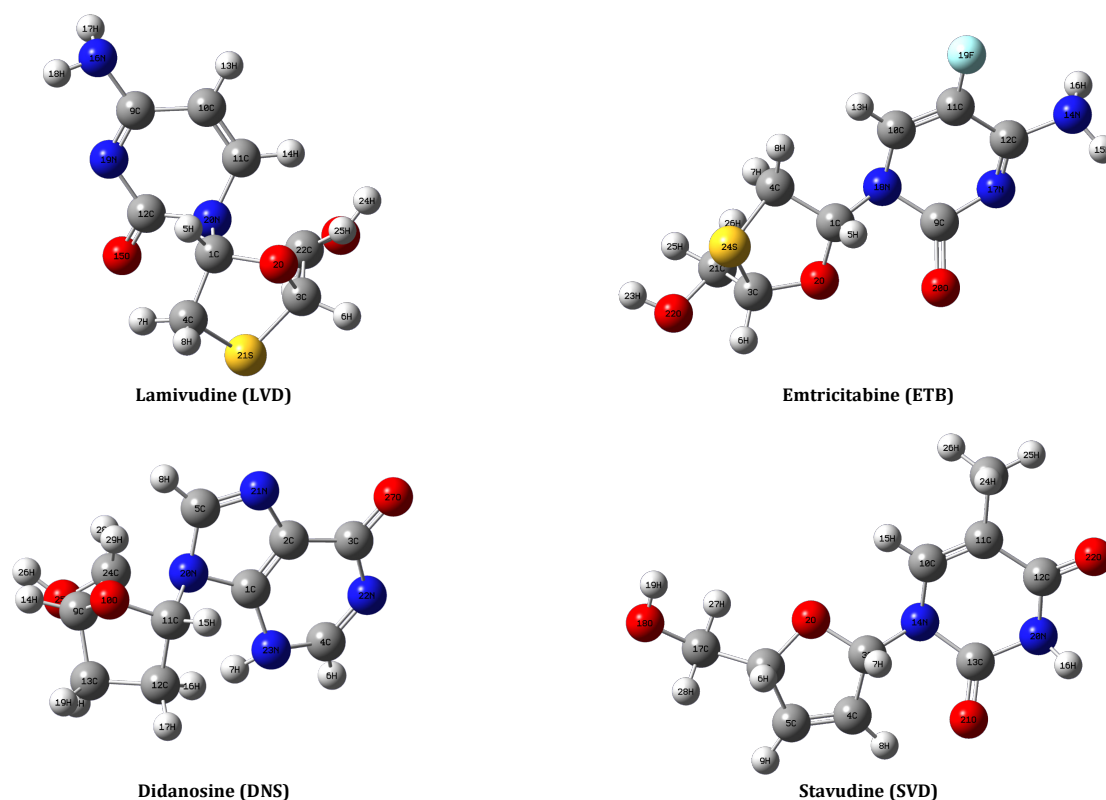


Figure 2. Optimized molecular structures of the neutral inhibitor molecules using B3LYP/6-31G(d).

$$\omega^+ = \frac{(I+3A)^2}{16(I-A)} \quad (10)$$

$$\omega^- = \frac{(3I+A)^2}{16(I+A)} \quad (11)$$

The fraction of electrons transferred ( $\Delta N$ ) from the inhibitor molecule to the metal was calculated according to the Pearson electronegativity scale [44], which states that for a reaction of two systems with different electronegativities, the electron flow will occur from the lower value system (inhibitor) to the higher value system (metal surface) until the chemical potentials are equal. The calculation was performed using the equation:

$$\Delta N = \frac{\chi_{Cu} - \chi_{inh}}{2(\eta_{Cu} + \eta_{inh})} \quad (12)$$

where  $\chi_{Cu}$  and  $\eta_{Cu}$ ,  $\chi_{inh}$  and  $\eta_{inh}$  denote the electronegativity and hardness of copper and the inhibitor molecule respectively. In our case we use the theoretical value of  $\chi_{Cu} = 4.98$  eV/mol and  $\eta_{Cu} = 0$  [45], for the calculation of the number of transferred electrons.

The Fukui functions were determined from Mulliken charges to locate the sites of reactivity within each molecule. These functions can be determined by using the finite difference approximation:

$$\text{Nucleophilic attack} \quad f_k^+ = q_k(N+1) - q_k(N) \quad (13)$$

$$\text{Electrophilic attack} \quad f_k^- = q_k(N) - q_k(N-1) \quad (14)$$

where  $q_k(N+1)$ ,  $q_k(N)$  and  $q_k(N-1)$  are the electronic population of atom  $k$  in  $(N+1)$ ,  $N$  and  $(N-1)$  electrons systems.

Recently, in order to precisely determine the sites of electrophilic and nucleophilic attack within the molecule, some

authors [46,47] have introduced the dual descriptor. This descriptor is expressed by the following relationship:

$$\Delta f_k(r) = \left( \frac{\partial f_k(r)}{\partial N} \right)_{v(r)} \quad (15)$$

The condensed form of the dual descriptor can be computed using the following equation:

$$\Delta f_k(r) = f_k^+ - f_k^- \quad (16)$$

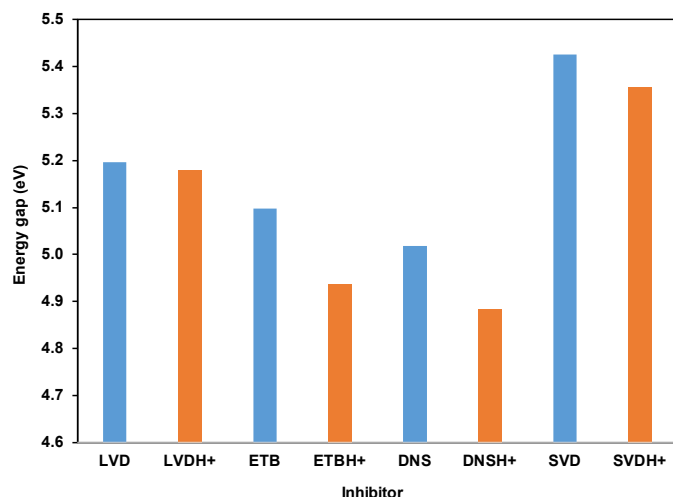
### 3. Results and discussion

#### 3.1. Quantum chemical assessment

The results of the optimization geometry of the selected molecules using B3LYP/6-31G(d) are presented in Figure 2. These optimized molecules provided access to the quantum chemical parameters for neutral and protonated form of inhibitors reported in Table 1. The acceptance of electrons from a metal by the inhibitor is influenced by its lowest unoccupied molecular orbital (LUMO), because it has the lowest energy, which facilitates the entry of new electrons. The highest occupied molecular orbital (HOMO) is a donor electron because it is the electron emission orbital, which is linked to the ionization potential [48-50]. Indeed, this electron donation occurs mainly during the distribution of the electron density over the entire molecule. However, the molecule may have the ability to receive electrons if the value of the lowest unoccupied molecular orbital energy (LUMO) is low and give electrons if the lowest unoccupied molecular orbital energy ( $E_{\text{HOMO}}$ ) is high [48-50]. The values obtained with neutral molecules are high and follow the trend: DNS > ETB > LVD > SVD, which implies that these molecules have a better electron donating propensity, therefore, a stronger adsorption on the copper surface and which leads to a higher inhibition efficiency.

**Table 1.** Computed quantum chemical parameters of neutral and protonated of selected molecules.

Parameters	LVD	LVDH <sup>+</sup>	ETB	ETBH <sup>+</sup>	DNS	DNSH <sup>+</sup>	SVD	SVDH <sup>+</sup>
$E_{\text{HOMO}}$ (eV)	-6.2476	-6.1924	-6.2124	-6.1902	-6.1390	-6.0806	-6.3912	-6.2006
$E_{\text{LUMO}}$ (eV)	-1.0511	-1.0122	-1.1149	-1.2530	-1.1215	-1.1962	-0.9659	-0.8427
$\Delta E$ (eV)	5.1965	5.1802	5.0975	4.9372	5.0175	4.8844	5.4253	5.3579
$\mu$ (D)	5.4800	4.0880	5.0085	4.3895	4.2281	3.6160	3.4619	3.2299
$I$ (eV)	6.2476	6.1924	6.2124	6.1902	6.1390	6.0806	6.3912	6.2006
$A$ (eV)	1.0511	1.0122	1.1149	1.2530	1.1215	1.1962	0.9659	0.8427
$\chi$ (eV)	3.6494	3.6023	3.6637	3.7216	3.6303	3.6384	3.6786	3.5832
$\eta$ (eV)	2.5983	2.5901	2.5488	2.4686	2.5088	2.4422	2.7127	2.6790
$\sigma$ (eV <sup>-1</sup> )	0.3849	0.3860	0.3923	0.4051	0.3986	0.4095	0.3686	0.3733
$\Delta N$	0.2561	0.2659	0.2582	0.2549	0.2690	0.2747	0.2399	0.2607
$\omega$	2.5629	2.5050	2.6332	2.8053	2.6266	2.7100	2.4942	2.3963
$\omega^+$	1.0629	1.0276	1.1199	1.2530	1.1250	1.1963	0.9940	0.8888
$\omega^-$	4.7122	4.6299	4.7825	4.9747	4.7553	4.8348	4.6725	4.4104

**Figure 3.** Energy gap ( $\Delta E$ ) diagram of the neutral and protonated forms of the tested molecules.

DNS with the highest  $E_{\text{HOMO}}$  value would adsorb more on the copper surface because of the disposition of the free electron pairs on the heteroatoms, hence its greater inhibition efficiency. It is also noted in our study that the  $E_{\text{LUMO}}$  values of the compounds studied are low, which shows that these molecules easily receive electrons from copper. The  $E_{\text{HOMO}}$  and  $E_{\text{LUMO}}$  values obtained with protonated molecules are relatively higher than those obtained with neutral molecules, suggesting that the protonation phenomenon increases the tendency of these inhibiting compounds to give and receive electrons from copper. Indeed, the protonation of an inhibitor leads to an increased nuclear charge, so the protonated molecules have a greater affinity for electron gain and donation. This donor-acceptor relationship between inhibitor molecules and metal orbitals promotes the formation of covalent bonds (chemisorption) and interactions between protonated species and  $\text{NO}_3^-$  ions adsorbed on copper surface (physisorption). It has been proven by some authors [51,52], that the best corrosion inhibitors are compounds that give electrons to an empty molecular orbital and receive free electrons from metal orbitals. Therefore, the molecules studied could be good inhibitors of copper.

The reactivity of a molecule and its capacity to be a good inhibitor is proven by the energy gap ( $\Delta E$ ). Moreover, the low value of energy gap of a molecule confirms its strong interaction on the metal surface [53], hence its high inhibition efficiency. The molecules studied have low energy gap values and these values are in the following order:  $\text{DNS} < \text{ETB} < \text{LVD} < \text{SVD}$  for neutral forms and  $\text{DNSH}^+ < \text{ETBH}^+ < \text{LVDH}^+ < \text{SVDH}^+$  for protonated forms. The values of  $\Delta E$  for the protonated forms are relatively lower than those obtained with the neutral forms. It results in the fact that the protonated molecules in nitric acid solution adsorb more on the copper surface creating a

protective layer that will isolate the copper from this aggressive medium. The trend shows that DNS with the lowest value of  $\Delta E$  (Figure 3) would be the best inhibitor.

The reactivity of a molecule also depends on its electronic affinity ( $A$ ) and its ionization potential ( $I$ ) [54]. In addition, a molecule with a low ionization energy value has a high reactivity. The different molecules studied have a low ionization energy value, which may reflect their better performance in inhibiting copper corrosion. The values of these parameters obtained with the protonated forms confirm their adsorption on the metal surface.

It is also documented in the literature [55,56] that higher values of dipole moment ( $\mu$ ) can lead to adsorption of the inhibitor creating a layer on the metal surface that would increase the inhibition efficiency. The dipole moments obtained with the neutral and protonated forms are high, which could justify the good adsorption of the molecules studied on the copper surface. However, other authors suggest that a high dipole moment value of organic compounds would favor a high inhibition [57,58], so in general this lack of consensus means that this indicator cannot be used in the prediction of the inhibitory activities of the molecules studied.

The adsorption of a molecule on a metal surface also derives from its capacity of attraction, it results in the fact that the capacity of attraction of the studied compounds is lower than copper because  $\chi_{\text{inh}} < \chi_{\text{Cu}}$  where  $\chi_{\text{Cu}} = 4.98$ , which suggests that the electrons of the molecules are more attracted by copper. The fraction of electrons transferred  $\Delta N < 0$ , less than 3.6 [58], and follows the trend  $\text{DNS} > \text{ETB} > \text{LVD} > \text{SVD}$ , which confirms the flow of electrons from molecules to copper, indicating that the molecules can donate electrons to copper surface, hence the formation of adsorptive bonds. As a result, this comparison indicates that DNS should be the best inhibitor.

**Table 2.** Calculated Mulliken atomic charges, Fukui function and dual descriptor of LVD neutral by B3LYP/6-31G(d).

Atoms	$q_k(N+1)$	$q_k(N)$	$q_k(N-1)$	$f_k^+$	$f_k^-$	$\Delta f_k(r)$
1 C	0.001585	0.192104	0.024981	-0.190519	0.167123	-0.357642
2 O	0.015360	-0.458681	0.007687	0.474041	-0.466368	0.940409
3 C	0.172646	-0.120426	0.003456	0.293072	-0.123882	0.416954
4 C	0.000966	0.416347	0.002608	0.417313	-0.418955	0.836268
5 H	0.001225	0.175902	-0.003387	-0.174677	0.179289	-0.353966
6 H	0.017233	0.178991	0.002741	-0.161758	0.176250	-0.338008
7 H	-0.000798	0.223743	0.000027	-0.224541	0.223716	-0.448257
8 H	-0.000557	0.194336	0.000285	-0.194893	0.194051	-0.388944
9 C	0.002129	0.389186	0.283716	-0.387057	0.105470	-0.492527
10 C	0.000849	-0.162568	-0.060548	0.163417	-0.102020	0.265437
11 C	0.011993	0.084585	0.243046	-0.072592	-0.158461	0.085869
<b>12 C</b>	0.000548	0.636756	0.130480	-0.636208	<b>0.506276</b>	<b>-1.142484</b>
13 H	0.000070	0.160433	0.002855	-0.160363	0.157578	-0.317941
14 H	0.000083	0.166729	-0.006753	-0.166646	0.173482	-0.340128
15 O	0.005097	-0.430196	0.159589	0.435293	-0.589785	1.025078
<b>16 N</b>	0.002777	-0.748305	-0.004267	<b>0.751082</b>	-0.744038	<b>1.495120</b>
17 H	0.000024	0.339846	0.010025	-0.339822	0.329821	-0.669643
18 H	0.000101	0.336720	0.002928	-0.336619	0.333792	-0.670411
19 N	0.002239	-0.455651	-0.000489	0.457890	-0.455162	0.913052
20 N	0.037916	-0.437003	-0.057849	0.474919	-0.379154	0.854073
21 S	0.015819	0.108085	0.009560	-0.092266	0.098525	-0.190791
22 C	0.323070	0.015035	0.118670	0.308035	-0.103635	0.411670
23 O	0.150044	-0.552794	0.037625	0.702838	-0.590419	1.293257
24 H	0.021748	0.324150	0.014535	-0.302402	0.309615	-0.612017
25 H	0.089185	0.106099	0.044143	-0.016914	0.061956	-0.078870
26 H	0.128851	0.149271	0.034337	-0.020420	0.114934	-0.135354

The chemical behaviour of the investigated molecules was evaluated by hardness ( $\eta$ ) and softness ( $\sigma$ ) parameters. These parameters provide information on the stability and reactivity of the molecules [59]. A reactive molecule has a high value of softness and a low value of hardness. The results presented in Table 1 show that the molecules studied are reactive. DNS with the highest softness value (0.3986 (eV<sup>-1</sup>)) and the lowest hardness value (2.5088 eV) could adsorb to copper more easily than other compounds, thus creating a physical barrier that would prevent corrosion. Accordingly, a hard molecule has a large energy gap and a soft molecule has a small energy gap [60], which implies that in the study of corrosion inhibitors and their capacity to bind to the metal surface, the inhibitors are considered as a soft base and the metal surface as a soft acid.

The electrophilicity index ( $\omega$ ) measures the propensity of a molecule to accept and give electrons [41]. This index has recently been reinforced by two indicators which are electron donor ability ( $\omega^-$ ) and electron acceptor ability ( $\omega^+$ ) [43]. In addition, this reactivity index depends not only on electron affinity (A), but also on potential ionization (I) expressed by Equation 9. These parameters improve upon the electronegativity ( $\chi$ ) and hardness terms by giving more exceptional implications to ionization potential (I) and electron affinity (A). In our work the values of ( $\omega^-$ ) and ( $\omega^+$ ) for the neutral and protonated forms (Table 1) show that  $\omega^+$  is closer to electron affinity (A) while  $\omega^-$  is not too close to ionization potential (I). It results that the molecules tested have a good capacity to accept electrons from the metal, which could enhance their absorptive capacity on the copper surface.

The total energy (TE) is the sum of internal potential and kinetic energy of the system(S) and it has been acquired via the expression:

$$TE[S] = V_{ext}[S] + T_S[S] + J[S] + E_{xc}[S] \quad (17)$$

where  $V_{ext}[S]$ : the External potential of the system;  $T_S[S]$ : is Kinetic energy of the fictitious system;  $J[S]$ : Coulombic repulsion;  $E_{xc}[S]$ : the exchange-correlation energy.

Metal-molecule interactions can be described by this parameter [61]. In our work, the optimization steps have permitted to determine the energy of each compound. We have plotted the energy evolution of the fifteen first steps for each neutral and protonated species in Figure 4.

Analysing Figure 4, we can see that the optimization steps depend on the molecular structure. As regards the neutral LVD molecule, it stabilizes from five steps with a minimum total energy of -1099.5645 Ha, whereas its protonated form LVDH<sup>+</sup> requires eleven steps with a minimum energy equal to -1100.69 Ha, this difference could be justified by the presence of the amino group in this molecule which stabilizes the neutral form more quickly. ETB molecule and its protonated form ETBH<sup>+</sup> stabilize at eleven and nine steps, respectively, with the respective minimum total energies of -1198.6491 and -1199.3226 Ha. This modification of the steps compared to the previous molecule could be due to the presence of fluorine in ETB. Indeed, fluorine, being more electronegative than the other atoms present in ETB will influence its protonation, in other words, fluorine can intervene in the process of corrosion inhibition. The neutral form of DNS requires nine steps (-833.4882 Ha) and the protonated form DNSH<sup>+</sup> requires twelve steps (-833.5438 Ha), this increase in the number of steps can be explained by the large molecular surface area with electrons  $\pi$  and heteroatoms in this molecule. These atoms have the strongest capacity to bind to the metal surface by promoting the adsorption of molecules to the copper surface. The methyl group present in SVD also promotes a gap between the neutral form which stabilizes at nine steps and the protonated form SVDH<sup>+</sup>, which needs ten steps to stabilize because this methyl group has the ability to donate electrons. This donation would contribute to the decrease of the total energy from -798.6734 Ha for SVD to -799.1848H for SVDH<sup>+</sup>. It is generally observed that the total energy decreases from the neutral to the protonated form which translates that the heteroatoms N, S, and O present in the different compounds have lonely electron pairs which are important for binding unfilled 3d orbitals of Cu<sup>2+</sup> ([Ar]3d<sup>9</sup>), ion; they thus determine the adsorption of the molecules on the copper surface. Similar results have been observed in the literature [62-64]. The total energy (TE) values of all the molecules studied are negative, which reveals that the transfer of charge to a molecule, followed by a backdonation from the molecule, is energetically favored [59]. In this context, the adsorption of inhibitors on the metal surface can occur spontaneously.

In order to predict the adsorption centers of inhibitor molecules which are likely sites for electrophilic and nucleophilic attack, Fukui functions and the dual descriptor were used.

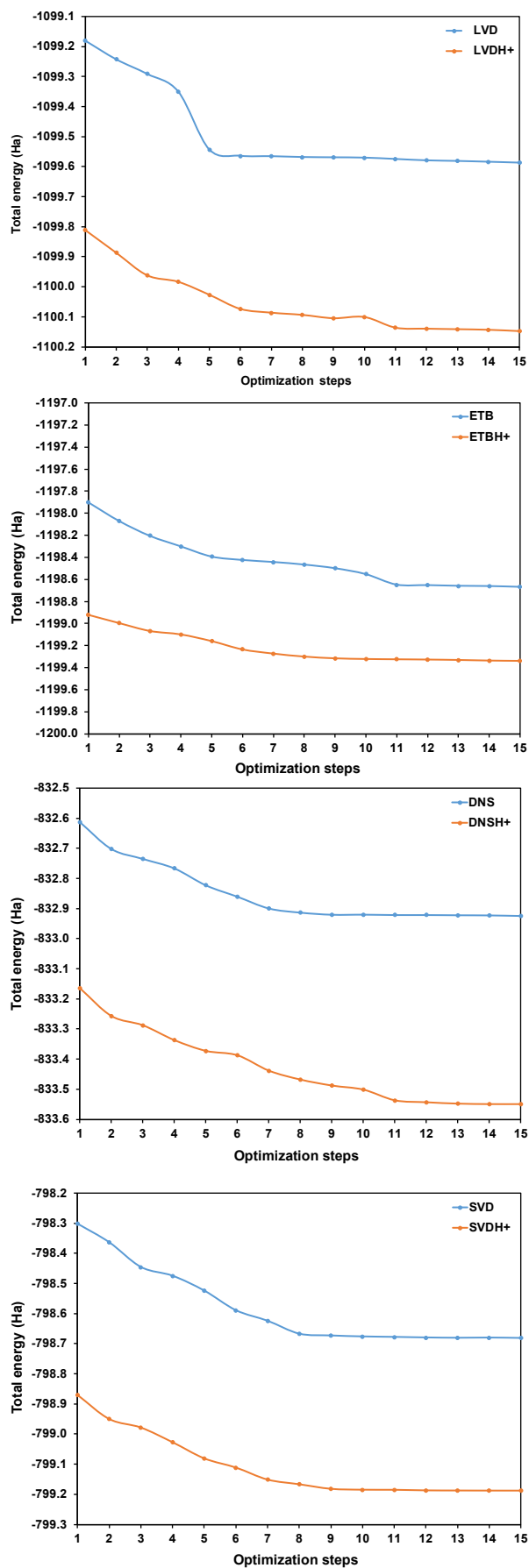


Figure 4. Total energy versus optimization steps of molecules studied in neutral and protonated forms.

**Table 3.** Calculated Mulliken atomic charges, Fukui function and dual descriptor of ETB neutral by B3LYP/6-31G(d).

Atoms	$q_k(N+1)$	$q_k(N)$	$q_k(N-1)$	$f_k^+$	$f_k^-$	$\Delta f_k(r)$
1 C	-0.003414	0.292999	0.003619	-0.296413	0.289380	-0.585793
2 O	0.032996	-0.461040	-0.004903	0.494036	-0.456137	0.950173
3 C	-0.039835	-0.069305	0.014961	0.029470	-0.084266	0.113736
4 C	0.009440	-0.519841	-0.000446	0.529281	-0.519395	1.048676
5 H	0.000570	0.183910	0.007060	-0.183340	0.176850	-0.360190
6 H	0.016948	0.232678	-0.003629	-0.215730	0.236307	-0.452037
7 H	-0.001711	0.240497	0.000923	-0.242208	0.239574	-0.481782
8 H	0.000572	0.192377	0.002213	-0.191805	0.190164	-0.381969
9 C	-0.009751	0.609099	0.047488	-0.618850	<b>0.561611</b>	<b>-1.180461</b>
10 C	0.000644	-0.042890	0.219781	0.043534	-0.262671	0.306205
11 C	0.000046	0.333884	-0.042788	-0.333838	0.376672	-0.710510
12 C	-0.001838	0.341909	0.235826	-0.343747	0.106083	-0.449830
13 H	-0.000091	0.182102	-0.012352	-0.182193	0.194454	-0.376647
14 N	0.002122	-0.729976	-0.007223	<b>0.732098</b>	-0.722753	<b>1.454851</b>
15 H	-0.000093	0.345621	0.005611	-0.345714	0.340010	-0.685724
16 H	-0.000056	0.340826	0.007385	-0.340882	0.333441	-0.674323
17 N	0.002667	-0.430648	0.086029	0.433315	-0.516677	0.949992
18 N	-0.000180	-0.440940	0.035124	0.440760	-0.476064	0.916824
19 F	0.000054	-0.271966	-0.001837	0.272020	-0.270129	0.542149
20 O	0.051932	-0.464075	0.040164	0.516007	-0.504239	1.020246
21 C	0.795466	-0.093373	0.262878	<b>0.888839</b>	-0.356251	<b>1.245090</b>
22 O	0.116210	-0.567308	0.039282	0.683518	-0.606590	1.290108
23 H	0.002993	0.368382	-0.001319	-0.365389	0.369701	-0.735090
24 S	0.025217	0.170138	0.033461	-0.144921	0.136677	-0.281598
25 H	-0.032567	0.147942	0.040066	-0.180509	0.107876	-0.288385
26 H	0.031660	0.108998	-0.007376	-0.077338	0.116374	-0.193712

**Table 4.** Calculated Mulliken atomic charges, Fukui function and dual descriptor of DNS neutral by B3LYP/6-31G(d).

Atoms	$q_k(N+1)$	$q_k(N)$	$q_k(N-1)$	$f_k^+$	$f_k^-$	$\Delta f_k(r)$
1 C	0.006865	0.443622	0.292496	-0.436757	0.151126	-0.587883
2 C	-0.003077	0.151606	-0.055610	-0.154683	0.207216	-0.361899
3 C	0.000401	0.524958	0.120746	-0.524557	<b>0.404212</b>	<b>-0.928769</b>
4 C	-0.000715	0.210861	0.175503	-0.211576	0.035358	-0.246934
5 C	-0.020063	0.211827	0.061412	-0.231890	0.150415	-0.382305
6 H	-0.000077	0.198435	-0.008480	0.198512	0.206915	-0.405427
7 H	0.000315	0.369233	0.007916	-0.368918	0.361317	-0.730235
8 H	-0.000156	0.210492	-0.003060	-0.210648	0.213552	-0.424200
9 C	0.047904	0.024327	0.083799	0.023577	-0.059472	0.083049
10 O	-0.004728	-0.500679	0.002158	0.495951	-0.502837	0.998788
11 C	-0.001923	0.275769	0.018475	-0.277692	0.257294	-0.534986
12 C	0.002747	-0.287542	0.001409	0.290289	-0.288951	0.579240
13 C	0.032609	-0.223333	-0.000455	-0.225942	-0.222878	0.478820
14 H	0.004075	0.150519	-0.000961	-0.146444	0.151480	-0.297924
15 H	0.002020	0.180196	-0.001746	-0.178176	0.181942	-0.360118
16 H	-0.000440	0.111676	-0.000603	-0.112116	0.112279	-0.224395
17 H	-0.000599	0.167456	0.000404	-0.168055	0.167052	-0.335107
18 H	-0.001545	0.167659	0.000201	-0.169204	0.167458	-0.336662
19 H	0.015980	0.147419	0.003101	-0.131439	0.144318	-0.275757
20 N	0.097085	-0.554478	-0.048084	0.651563	-0.506394	1.157957
21 N	0.075712	-0.429451	0.041578	0.505163	-0.471029	0.976192
22 N	0.001263	-0.433056	-0.061921	0.434319	-0.371135	0.805454
23 N	0.002966	-0.635684	0.051925	0.638650	-0.687609	1.326259
24 C	0.461186	-0.100770	-0.033232	0.561956	-0.067538	0.629494
25 O	0.114798	-0.604475	0.041974	<b>0.719273</b>	-0.646449	<b>1.365722</b>
26 H	0.030308	0.340277	-0.002449	-0.309969	0.342726	-0.652695
27 O	-0.001584	-0.454763	0.146654	0.453179	-0.601417	1.054596
28 H	0.031727	0.160873	0.114859	-0.129146	0.046014	-0.175160
29 H	0.106944	0.177028	0.051990	-0.070084	0.125038	-0.195122

Thus, the atomic sites favoured for nucleophilic attack have a high value of  $f_k^+$  and a positive dual descriptor ( $\Delta f_k(r)$ ) (highest value), while those favored for electrophilic attack have a negative dual descriptor (lowest value) and a high value of  $f_k^-$ . Tables 2-5 present Mulliken charge values, Fukui functions and the dual descriptor of each inhibitor. The nucleophilic attack sites of a molecule have a strong tendency to receive electrons and are therefore linked to the LUMO orbitals, while the electrophilic attack sites have a capacity to give electrons and are associated with the HOMO orbitals. The HOMO and LUMO diagrams of each inhibitor are shown in Figure 5.

As can be seen from the calculations, it is clear that the probable site for nucleophilic attack of LVD is N(16) and the electrophilic attack is C(12). For ETB, nucleophilic attack centre is controlled by N (14) because C(21) carbon atom with the highest value of  $f_k^+$  does not have the highest value of  $\Delta f_k(r)$

while the electrophilic attack centre is controlled by C(9). In table 4, O(25) and C(3) are respectively the most susceptible sites of nucleophilic and electrophilic attack for DNS. The nucleophilic attack centre for SVD is governed by C(17) and the electrophilic centre of attack is indicated by C(13).

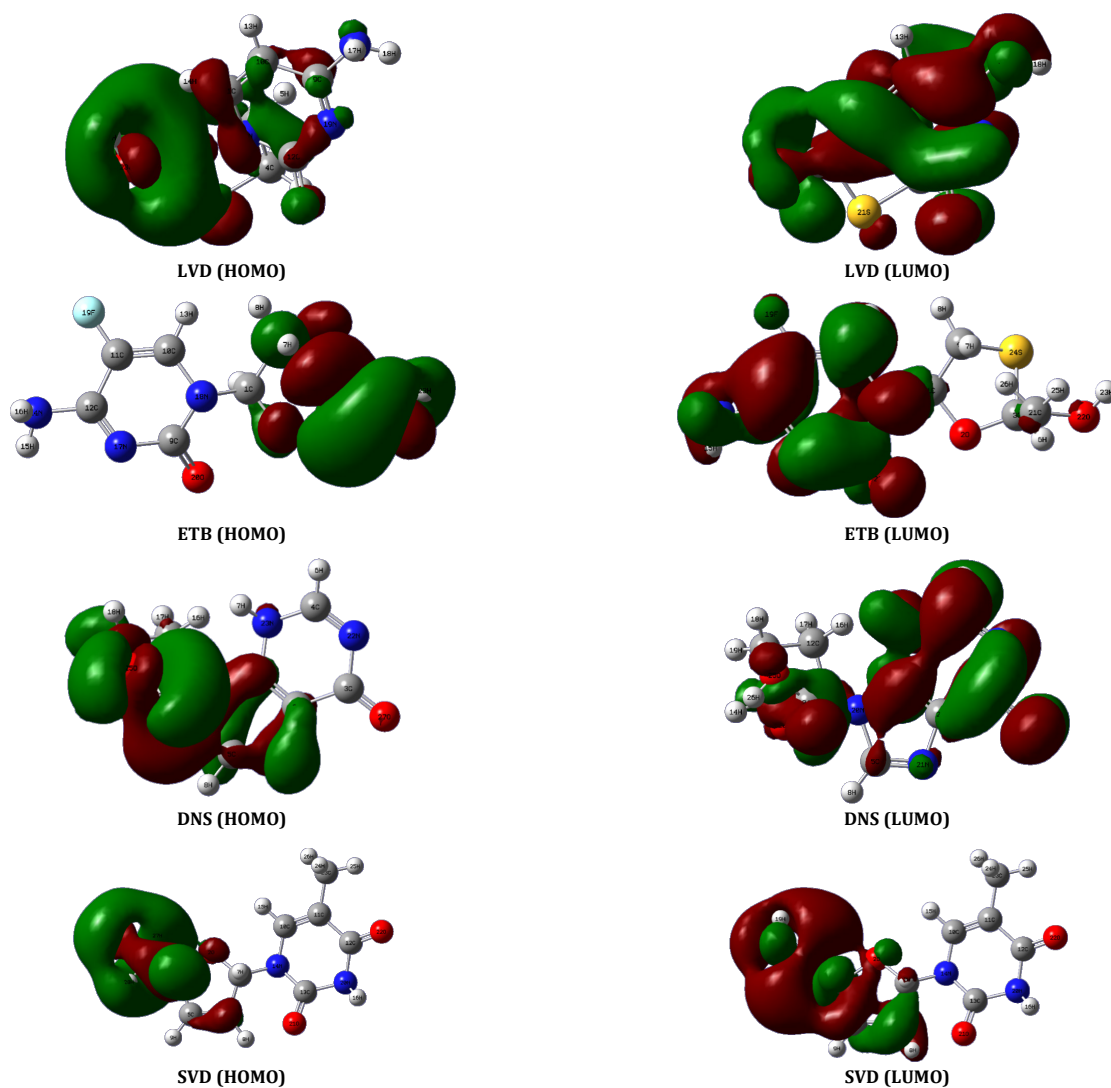
### 3.2. Inhibition mechanism

After the analysis of the quantum chemical parameters, it appears that the inhibition mechanism requires a full knowledge of the interaction between the inhibitor and the metal surface. In nitric acid solution, inhibitors that are antiretrovirals (ARV) will be protonated according to the equation:



**Table 5.** Calculated Mulliken atomic charges, Fukui function and dual descriptor of SVD neutral by B3LYP/6-31G(d).

Atoms	$q_k(N+1)$	$q_k(N)$	$q_k(N-1)$	$f_k^+$	$f_k^-$	$\Delta f_k(r)$
1 C	0.053094	0.025118	-0.048602	0.027976	0.073720	-0.045744
2 O	0.003478	-0.526316	0.008144	0.529794	-0.534460	1.064254
3 C	-0.003160	0.256748	0.004065	-0.259908	0.252683	-0.512591
4 C	0.018056	-0.110318	0.035117	0.128374	-0.145435	0.273809
5 C	0.000698	-0.125546	0.025200	0.126244	-0.150746	0.276990
6 H	0.056513	0.134242	0.016376	-0.077729	0.117866	-0.195595
7 H	-0.000049	0.160487	0.007429	-0.160536	0.153058	-0.313594
8 H	-0.000957	0.200462	-0.000025	-0.201419	0.200487	-0.401906
9 H	0.000272	0.160991	-0.001545	-0.160719	0.162536	-0.323255
10 C	0.000611	-0.015524	0.223885	0.016135	-0.239409	0.255544
11 C	0.002960	0.070888	-0.005346	-0.067928	0.076234	-0.144162
12 C	-0.000921	0.503955	0.131359	-0.504876	0.372596	-0.877472
<b>13 C</b>	<b>0.000098</b>	<b>0.692052</b>	<b>0.000664</b>	<b>-0.691954</b>	<b>0.691388</b>	<b>-1.383342</b>
14 N	0.000131	-0.483862	-0.003212	0.483993	-0.480650	0.964643
15 H	-0.000005	0.195188	-0.013139	-0.195193	0.208327	-0.403520
16 H	-0.000018	0.364432	0.003758	-0.364450	0.360674	-0.725124
<b>17 C</b>	<b>0.775103</b>	<b>-0.067360</b>	<b>0.435773</b>	<b>0.842463</b>	<b>-0.503133</b>	<b>1.345596</b>
18 O	0.126262	-0.567983	0.067916	0.694245	-0.635899	1.330144
19 H	0.006859	0.356981	-0.007787	-0.350122	0.364768	-0.714890
20 N	0.000070	-0.599383	0.007638	0.599453	-0.607021	1.206474
21 O	0.000602	-0.486901	0.002037	0.487503	-0.488938	0.976441
22 O	0.002110	-0.483823	0.085469	0.485933	-0.569292	1.055225
23 C	-0.000143	-0.509074	-0.001119	0.508931	-0.507955	1.016886
24 H	0.000232	0.177342	0.000340	-0.177110	0.177002	-0.354112
25 H	0.000059	0.194565	-0.000435	-0.194506	0.195000	-0.389506
26 H	0.000043	0.164844	0.002011	-0.164801	0.162833	-0.327634
27 H	-0.013129	0.142604	0.002157	-0.155733	0.140447	-0.296180
28 H	-0.027666	0.175192	0.021872	-0.202858	0.153320	-0.356178

**Figure 5.** HOMO and LUMO diagram of neutral molecules investigated.

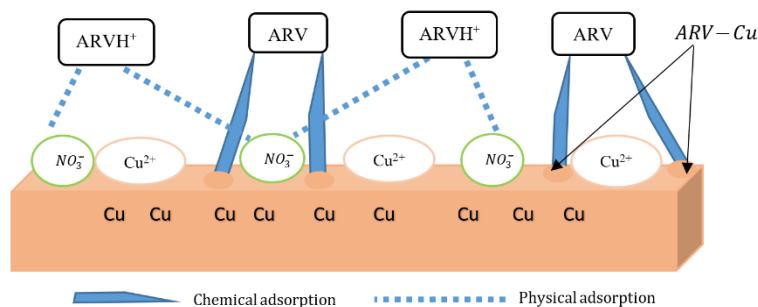


Figure 6. Schematic representation of adsorption of ARV on copper surface in 1.0 M HNO<sub>3</sub>.

These protonated inhibitors are positively charged, so interactions are created between its protonated species and the NO<sub>3</sub><sup>-</sup> ions adsorbed on the metal surface reflect the physical adsorption. The studied inhibitors contain heteroatoms (oxygen, nitrogen, and sulphur) and π-electrons, which participate in the formation of covalent bonds with the electrons of the copper empty orbitals; that is chemical adsorption. These two phenomena are justified by the values of ΔN and ω of the different molecules studied. These different transformations will favor the formation of a complex (inh-Cu) that will cover the surface of the metal by isolating it from nitric acid. This formation is summarized by the following reaction:



The mechanism proposed in our case is shown in Figure 6.

#### 4. Conclusion

The computational approach has shown that the four eco-friendly compounds, LVD, ETB, DNS and SVD could have remarkable inhibition properties of copper corrosion in nitric acid solution. Furthermore, DNS would have the best inhibition performance due to the heteroatoms disposition and its large molecular surface area. They have the ability to give or receive electrons from the unfilled orbitals of copper. However, the electron acceptor ability value (ω<sup>+</sup>) proves that these molecules are more acceptors than donors, which allows them to inhibit copper corrosion. It also results that the total energy (TE) of these compounds decreases when they are protonated in an acidic medium, thus showing their capacity to form covalent bonds with copper. The presence of free electron pairs on the heteroatoms or π electrons can strongly contribute to the adsorption process on the metal surface. From the local reactivity indices, it was found that the nucleophilic attack sites for LVD, ETB, DNS and SVD are N(16), N(14), O(25) and C(17) respectively, while the electrophilic attack sites are denoted by C(12), C(9), C(3) and C(13). Finally, these compounds may be good inhibitors of metal corrosion.

#### Acknowledgements

The authors gratefully acknowledged the support of Environmental Training and Research Unit of Jean Lorougnon Guédé University of Daloa, Côte d'Ivoire and The Laboratory of Physical Chemistry of Felix Houphouët Boigny University of Abidjan, Côte d'Ivoire.

#### Disclosure statement

Conflict of interests: The authors declare that they have no conflict of interest.

Author contributions: All authors contributed equally to this work.

Ethical approval: All ethical guidelines have been adhered.

Sample availability: Samples of the compounds are available from the author.

#### ORCID

Mougo André Tigori

<http://orcid.org/0000-0002-3722-7896>

Amadou Kouyaté

<http://orcid.org/0000-0002-4102-5891>

Victorien Kouakou

<http://orcid.org/0000-0003-0716-8466>

Paulin Marius Niamien

<http://orcid.org/0000-0002-0744-9623>

Albert Trokourey

<http://orcid.org/0000-0001-7139-5976>

#### References

- Ozcan, M.; Solmaz, R.; Kardas, G.; Dehri, I. *Colloids Surf. A* **2008**, *325*, 57-63.
- Scendo, M.; Hepel, M. *J. Electroanal. Chem.* **2008**, *613*, 35-50.
- Laggoun, R.; Ferhat, M.; Saidat B.; Ali Benghia A.; Chaabani A. *Corros. Sci.* **2020**, *165*, 1-39.
- Padash, R.; Sajadi, G. S.; Jafari, A. H.; Jamalizadeh, E.; Shokuhi, R. A. *Mater. Chem. Phys.* **2020**, *244*, 122681.
- Deyab, M. A. *J. Mol. Liq.* **2020**, *309*, 113107.
- Antonijevic, M. M.; Petrovic, M. B. *Int. J. Electrochem. Sci.* **2008**, *3*, 1-28.
- Deyab, M. A. *J. Ind. Eng. Chem.* **2015**, *25*, 384-389.
- Pirvu, L.; Neagu, G.; Terchescu, I.; Albu, B.; Stefanu, A. *Open Chem.* **2020**, *18*, 488-502.
- Shahraki, M.; Habibi-Khorassani, S. M.; Noroozifar, M.; Yavari, Z.; Darjani, M.; Dehdab, M. *Iran. J. Mater. Sci. Eng.* **2017**, *14*, 35-47.
- Tamborim, S. M.; Dias, S. L. P.; Silva, S. N.; Dick, L. F. P.; Azambuja, D. S. *Corros. Sci.* **2011**, *53*, 1571-1580.
- Prabhu, R. A.; Shanbhag, A. V.; Venkatesha, T. V. *J. Appl. Electrochem.* **2007**, *37*, 491-497.
- Shylesha, B. S.; Venkatesha, T. V.; Praveen, B. M. *J. Chem. Pharm. Res.* **2011**, *3*, 501-507.
- Abdallah, M.; Zaafarany, I.; Al-Karane, S. O.; Abd El-Fattah, A. A. *Arabian J. Chem.* **2012**, *5*, 225-234.
- Fouda, A. S.; El-Ewady, G. Y.; Shalabi, K. J. *Korean Chem. Soc.* **2011**, *55*, 268-278.
- Ebenso, E. E.; Obot, I. B. *Int. J. Electrochem. Sci.* **2010**, *5*, 2012-2035.
- Reza, I.; Saleemi, A. R.; S. Naveed, S. *Polish J. Chem. Tech.* **2011**, *13*, 67-71.
- Tigori, M. A.; Kouyate, A.; Assouma, D. C.; Kouakou, V.; Niamien, P. M. *Am. J. Mater. Sci. Eng.* **2020**, *8*, 6-16.
- Abdallah, M.; azosulpha, R. *Corros. Sci.* **2002**, *44*, 717-728.
- Ebenso, E. E.; Arslan, T.; Kandemirli, F.; Caner, N.; Love, I. *Int. J. Quantum Chem.* **2010**, *110*, 1003-1018.
- Verma, C.; Haque, J.; Quraishi M. A.; Ebenso, E. E. *J. Mol. Liq.* **2019**, *275*, 18-40.
- Zulfareen, N.; Venugopal T.; Kannan. K. *Int. J. Corros.* **2018**, *2018*, 9372804, 1-18.
- Chauhan, D. S.; Ansari, K. R.; Sorour, A. A.; Quraishi, M. A.; Lgaz, H.; Salghi. R. *Int. J. Biol. Macromol.* **2018**, *107*, 1747-1757.
- Azzaoui, K.; Mejdoubi, E.; Jodeh, S.; Lamhamdi, A.; Castellon, E. R.; Algarra, M.; Zarrouk, A.; Errich, A.; Salghi R.; Hassane L. G. *Corros. Sci.* **2017**, *129*, 70-81.
- Kayadibi, F.; Zor, S.; Sagdinc, S. G. *Prot. Met. Phys. Chem. Surf.* **2016**, *52*, 356-371.

- [25]. Qiang Y.; Zhang, S.; Xu, S.; Li, W. *J. Colloid Interface Sci.* **2016**, *472*, 52-59.
- [26]. Fatima, S.; Sharma, R.; Asghar, F.; Kamal, A.; Badshah, A.; Kraatz, H. B. *J. Ind. Eng. Chem.* **2019**, *76*, 374-387.
- [27]. Ozturk, S. *Prot. Met. Phys. Chem. Surf.* **2018**, *545*, 953-962.
- [28]. Zhang, D.; Gao, L.; Zhou, G. *Corros. Sci.* **2004**, *46*, 3031-3040.
- [29]. Padash, R.; Rahimi-Nasrabadi, M.; Shokuhi Rad, A. *Appl. Phys. A* **2019**, *125*, 78, 1-11.
- [30]. Kumar, D.; Jain, N. V.; Rai, B. *Appl. Surf. Sci.* **2020**, *514*, 145905.
- [31]. Guo L.; Kaya, S.; Obot, I. B.; Zheng, X.; Qiang, Y. *J. Colloid Interface Sci.* **2017**, *506*, 478-485.
- [32]. Mo, S.; QunLuo, H.; Li, N. B. *J. Colloid Interface Sci.* **2017**, *505*, 929-939.
- [33]. Obot, I. B.; Macdonald, D. D.; Gasem, Z. M. *Corros. Sci.* **2015**, *99*, 1-30.
- [34]. Elmsellem, H.; Harit, T.; Aouniti, A.; Malek, F.; Riahi, A.; Chetouani, A.; Hammouti, B. *Prot. Met. Phys. Chem. Surf.* **2015**, *51*, 873-884.
- [35]. Guo, L.; Dong, W.; Zhang, S. *RSC Adv.* **2014**, *4*, 41956-41967.
- [36]. John, S.; Joy, J.; Prajila, M.; Joseph, A. *Mater. Corros.* **2011**, *62*, 1031-1041.
- [37]. Frisch, M. J.; Trucks, G. W.; Schlegel, H. B.; Scuseria, G. E.; Robb, M. A.; Cheeseman, J. R.; Scalmani, G.; Barone, V.; Mennucci, B.; Petersson, G. A.; Nakatsuji, H.; Caricato, M.; Li, X.; Hratchian, H. P.; Izmaylov, A. F.; Bloino, J.; Zheng, G.; Sonnenberg, J. L.; Hada, M.; Ehara, M.; Toyota, K.; Fukuda, R.; Hasegawa, J.; Ishida, M.; Nakajima, T.; Honda, Y.; Kitao, O.; Nakai, H.; Vreven, T.; Montgomery, Jr.; Peralta, J. E.; Ogliaro, F.; Bearpark, M.; Heyd, J. J.; Brothers, E.; Kudin, K. N.; Staroverov, V. N.; Kobayashi, R.; Normand, J.; Raghavachari, K.; Rendell, A.; Burant, J. C.; Iyengar, S. S.; Tomasi, J.; Cossi, M.; Rega, N.; Millam, J. M.; Klene, M.; Knox, J. E.; Cross, J. B.; Bakken, V.; Adamo, C.; Jaramillo, J.; Gomperts, R.; Stratmann, R. E.; Yazyev, O.; Austin, A. J.; Cammi, R.; Pomelli, C.; Ochterski, J. W.; Martin, R. L.; Morokuma, K.; Zakrzewski, V. G.; Voth, P.; Salvador, G. A.; Dannenberg, S. Dapprich, J. J.; Daniels, A. D.; Farkas, Ö.; Foresman, J. B.; Ortiz, J. V.; Cioslowski, J.; Fox, A. D. *J. Gaussian 09*. Gaussian, Inc., Wallingford, CT, 2009.
- [38]. Hohenberg, P.; Kohn, W. *Phys. Rev. B* **1964**, *136*, 864-887.
- [39]. Lee, C.; Yang, W.; Parr, R. G. *Phys. Rev. B* **1988**, *37*, 785-789.
- [40]. Koopmans, T. *Atoms Physica.* **1934**, *1*, 104-113.
- [41]. Parr, R. G.; Szentpaly, L. V.; Liu, S. *J. Am. Chem. Soc.* **1999**, *121*, 1922-1924.
- [42]. Yang, W.; Parr, R. G. *Proc. Natl. Acad. Sci.* **1986**, *83*, 8440-8441.
- [43]. Gazquez, J. L.; Cedillo, A.; Vela, A. *J. Phys. Chem. A* **2007**, *111*, 1966-1970.
- [44]. Pearson, R. G. *Inorg. Chem.* **1988**, *27*, 734-740.
- [45]. Michaelson, H. B. *J. Appl. Phys.* **1977**, *48*, 4729-4733.
- [46]. Martinez-Araya, J. I. *J. Math. Chem.* **2015**, *53*, 451-465.
- [47]. Morell, C.; Grand, A.; Toro Labbe, A. *J. Phys. Chem. A* **2004**, *109*, 205-212.
- [48]. Lebrini, M.; Traisnel, M.; Lagrenee, M.; Mernari, B.; Bentiss, F. *Corros. Sci.* **2008**, *50*, 473-479.
- [49]. Yurt, A.; Ulutas, S.; Dal, H. *Appl. Surf. Sci.* **2006**, *253*, 919-925.
- [50]. Xiao-Ci, Y.; Hong, Z.; Ming-Dao, L.; Hong-Xuan, R.; Lu-An, Y. *Corros. Sci.* **2000**, *42*, 645-653.
- [51]. Awad, M. K.; Mustafa, M. R.; Abo Elnga, M. M. *J. Mol. Struct. Theochem.* **2010**, *959*, 66-74.
- [52]. Fernandes, C. M.; Mello, M. V. P.; Santos, N. E. D.; Souza, A. M. T.; Lanznaster, M.; Ponzio, E. A. *Mater. Corros.* **2019**, *71*, 280-291.
- [53]. El Faydy, M.; Benhiba, F.; About, H.; Kerroum, Y.; Guenbour, A.; Lakhrissi, B.; Warad, I.; Verma, C.; El-Sayed M. S.; Ebnso, E. E.; Zarrrouk, A. *J. Colloid Interface Sci.* **2020**, *576*, 330-344.
- [54]. Chakraborty, T.; Gazi, K.; Ghosh, D. C. *Mol. Phys.* **2010**, *108*, 2081-2092.
- [55]. Quraishi, M.; Sardar, R. *J. Appl. Electrochem.* **2003**, *33*, 1163-1168.
- [56]. Pavithra, M. K.; Venkatesha, T. V.; Punith Kumar, M. K. *Int. J. Electrochem.* **2013**, *2013*, 1-9.
- [57]. Obot, I. B.; Gasem, Z. M. *Corros. Sci.* **2014**, *83*, 359-366.
- [58]. Lukovits, I.; Kalman, E.; Zucchi, F. *Corros.* **2011**, *57*, 3-8.
- [59]. Hegazy, M. A.; Atlam, F. M. *J. Mol. Liq.* **2016**, *218*, 649-662.
- [60]. Koch, E. C. *Explos. Pyrotech.* **2005**, *30*, 5-16.
- [61]. Gomez, B.; Likhanova, N. V.; Dominguez-Aguilar, M. A.; Martinez-Palou, R.; Vela, A.; Gazquez, J. L. *J. Phys. Chem. B* **2006**, *110*, 8928-8934.
- [62]. Obot, I. B.; Gasem, Z. M. *Corros. Sci.* **2014**, *83*, 359-366.
- [63]. El Faydy, M.; Benhiba, F.; About, H.; Kerroum, Y.; Guenbour, A.; Lakhrissi, B.; Warad, I.; Verma, C.; El-Sayed M. S.; Ebnso, E. E.; Zarrrouk, A. *J. Colloid Interface Sci.* **2020**, *576*, 330-344.
- [64]. Obot, I. B.; Umoren, S. A.; Gasem, Z. M.; Suleiman, R.; El Ali, B. *J. Ind. Eng. Chem.* **2015**, *21*, 1328-1329.



Copyright © 2020 by Authors. This work is published and licensed by Atlanta Publishing House LLC, Atlanta, GA, USA. The full terms of this license are available at <http://www.eurjchem.com/index.php/eurjchem/pages/view/terms> and incorporate the Creative Commons Attribution-Non Commercial (CC BY NC) (International, v4.0) License (<http://creativecommons.org/licenses/by-nc/4.0>). By accessing the work, you hereby accept the Terms. This is an open access article distributed under the terms and conditions of the CC BY NC License, which permits unrestricted non-commercial use, distribution, and reproduction in any medium, provided the original work is properly cited without any further permission from Atlanta Publishing House LLC (European Journal of Chemistry). No use, distribution or reproduction is permitted which does not comply with these terms. Permissions for commercial use of this work beyond the scope of the License (<http://www.eurjchem.com/index.php/eurjchem/pages/view/terms>) are administered by Atlanta Publishing House LLC (European Journal of Chemistry).